

Viscosity Measurement Technique for Long Fiber Thermoplastic Material

M. Kalaidov^{1*}, G. Meirson^{1**}, N. Heer^{1***}, Y. Fan^{*2}, S. Ivanov^{1****}, V. Ugresic^{1*****}, J. Wood^{**2},
A. Hrymak³

¹*Fraunhofer Project Centre for Composites Research, 2544 Advanced Ave, London, Ontario, Canada N6M 0E1*

Email: maksym.kalaidov@gmail.com **Email: gmeirson@uwo.ca *Email: nheer2@uwo.ca*

*****Email: sivanov@uwo.ca *****Email: yugresi@uwo.ca*

²*Department of Mechanical and Materials Engineering, University of Western Ontario, London, Ontario, Canada
N6A 5B9*

**Email: yfan4@uwo.ca **Email: jtwood@uwo.ca*

³*Department of Chemical and Biochemical Engineering, University of Western Ontario, London, Ontario, Canada*

Email: ahrymak@uwo.ca

Abstract

Long Fiber Thermoplastic-Direct (LFT-D) is gaining traction within the automotive industry as a cost-efficient manufacturing method for light-weight structural components. A key element required for the accurate prediction of the flow of the LFT-D material during molding is the material's viscosity. The present study proposes a new method for the fast calculation of LFT-D material viscosity in a squeeze flow environment and compares the results obtained by this method to known values. The measured viscosity could be used to improve process simulation.

Key words: LFT-D, viscosity, squeeze flow, simulation

1. Introduction

Design, processing, and production with fiber reinforced plastics (FRP) are part of the most ambitious and fastest-growing branches of engineering. Their increased popularity is primarily attributable to the extraordinary mechanical and physical properties of these materials, such as specific stiffness, impact resistance, strength, anisotropy, heat resistance, insulating ability, and many others [1]. The wide range of their applications and the variety of properties of the materials themselves make them relevant and sought-after subjects of study.

Each of the methods for producing parts from combinations of different groups of matrix materials such as thermosets, thermoplastics, and elastomers with numerous types of fibres such as carbon, aramid, glass, and others have their advantages and disadvantages and therefore find their use in different industry fields. Thus, in the automotive industry, the greatest challenges, besides the already mentioned desired mechanical and physical properties, are production cycle time, cost, quality and reproducibility of parts. One of the most suitable methods for meeting those requirements in the modern automotive industry is the Long Fiber Thermoplastic-Direct process (LFT-D).

Possible alternatives to this process are injection moulding, glass-mat reinforced thermoplastic sheets (GMT) or Long Fiber Thermoplastic-Granules (LFT-G). The main advantages of the LFT-D process over other methods are its simplicity, cycle time, freedom in design and the maximum weight of the parts produced. In addition, the process is easy to automate, which significantly reduces overall costs. Moreover, the technology avoids the step of producing, storage and transport of semi-finished products, compared to GMT or LFT-G processes [2].

The LFT-D process makes use of two twin screw extruders and a press. The first extruder is mixing the neat polymer with additives such as coloring agents or antioxidants. The mixture flows directly into the second extruder which also pulls in continuous fibers. The second extruder mixes the polymer and the fibers while breaking the fibers. As a result the second extruder produces a charge of mixed polymer and fibers that is moved into the press while it is still hot to be compressed into the final part. A schematic representation of the LFT-D machine equipment is given in Figure 1.

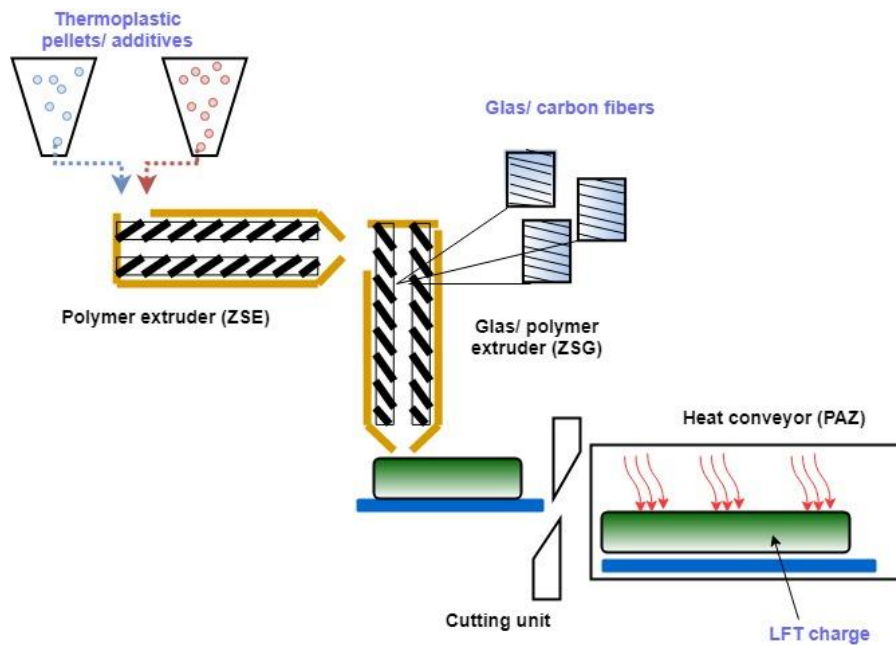


Figure 1: Schematic representation of the LFT-D process

Modern product development process includes three main steps: virtual prototyping, testing (including numerical simulation (e.g. finite element method, computational fluid mechanics)), and finally a pilot run. Precise calculations and simulation results are responsible for enormous cost reductions in the design process, avoiding unnecessary physical, process parameter, and material study. Therefore, accurate measurement methods for material property evaluation are increasingly gaining importance for industry applications. One significant problem of all these measurement methods is their complexity. Additionally, the rheological characterization of squeeze flow between parallel plates is still a challenge.

Compared to Newtonian behaviour, non-Newtonian viscosity is not a constant value and depends on the shear ratio (Bingham fluid, viscoplastic, pseudoplastic or dilatant fluids) and the duration of time over which the shear stress is applied to the fluid (thixotropic and rheopectic behaviours). Non-Newtonian

fluids, whose behaviour does not exhibit time-dependency belong to the group of generalized Newtonian fluids.

Since there is no uniform type of characterization for all fluids, different approximation models can be applied to describe their behaviour. Some of the most common are [3-6]:

- Power-law fluid
- Carreau fluid
- Bingham fluid
- Hershel-Bulkley fluid and others

Additional investigation has shown that the power-law model and the Carreau fluid model fit well to LFT-D type material.

The power-law model is believed to be a good approximation for a wide range of fluids [4]. It relates the shear stress and the shear rate of fluid flow in the following way:

$$\eta(\dot{\gamma}) = K\dot{\gamma}^{n-1}, \quad (1)$$

where K is the consistency parameter and n is the dimensionless power-law exponent.

The Carreau model, on the other hand, although more realistic [4], is also more complicated:

$$\eta(\dot{\gamma}) = \eta_{\infty} + (\eta_0 - \eta_{\infty})[1 + (\lambda\dot{\gamma})^2]^{\frac{n-1}{2}}, \quad (2)$$

where η_{∞} is the infinite-shear-rate-viscosity, η_0 is the zero-shear-rate-viscosity, λ is the relaxation time and n is the exponent. This model considers the fluid behavior as Newtonian for very low and very high shear rates, whereas it is similar to the power-law model for mid-range shear rates. The parameter λ indicates the transition from constant viscosity to the power-law region.

2. *Methods*

To obtain the data for the viscosity measurement, an LFT-D charge is placed in a mold and compressed while the data for force build-up, speed, and ram location is collected. A sketch of the experimental setup is given in Figure 2.

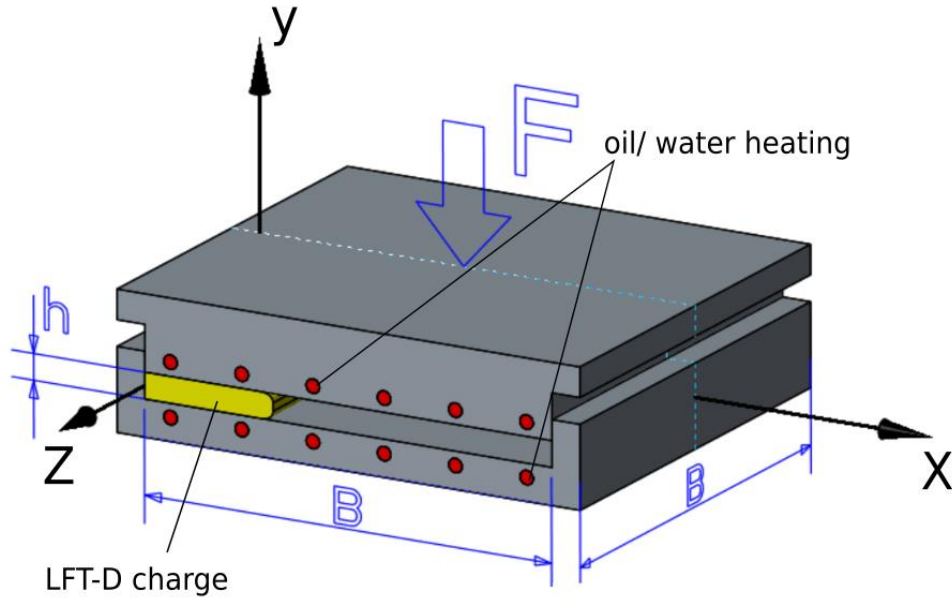


Figure 2: Experimental setup

In order to simplify the data analysis, several assumptions must be made:

- 1) Plastic melt is an incompressible fluid.
- 2) Elasticity effects are of no real consequence.
- 3) The problem is isothermal.
- 4) The compression speed is low enough to consider inertia effects as negligible.
- 5) Shear rate and wall shear stress values are taken at the edge of material front
- 6) The material flow description is considered to be one-dimensional problem. Hence, important boundary conditions are:
 - There is no flow in z-direction
 - There is no flow at $x=0$: $v(0, y) = 0$
 - There is no slip at walls: $v(x, \pm \frac{h}{2}) = 0$

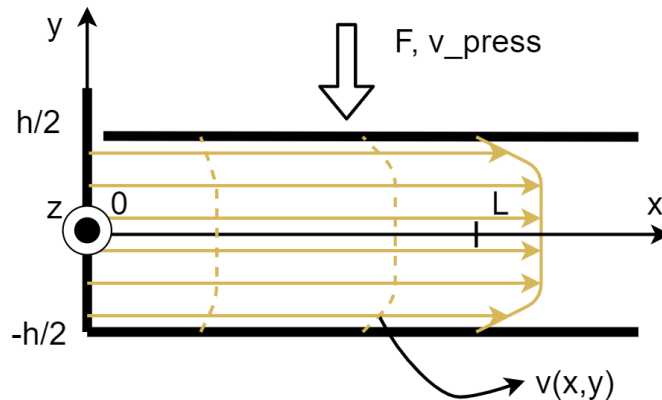


Figure 3: Boundary conditions of the problem

2.1 Shear stress

Using the similarity of press and slit rheometry methods [7], the magnitude of the wall shear stress τ_w can be defined as:

$$\tau_w = \left| \frac{h}{2(1 + h/B)} \frac{dp}{dx} \right| \quad (3)$$

Where, $\frac{dp}{dx}$ is the gradient of the hydrostatic pressure along x -direction, B is the mould width and h is the height of the gap between lower and upper halves (height of the charge). Since $B \gg h$, the relation can be simplified as:

$$\tau_w = \left| \frac{h}{2} \frac{dp}{dx} \right| \quad (4)$$

Although Eq. 3 is a simple expression, calculating the pressure gradient may be challenging. While slit and capillary rheometry methods consider the material flow as a fully developed steady flow, it is not the case for press squeeze flow due to the continuously changing gap height and press speed. To simplify the problem, we assume that most of the pressure drop is happening at the flow front.

In fact, a similar effect occurring during injection moulding of amorphous polymers was investigated by Mavridis, Hrymak and Vlachopoulos [8] as well as by Kamal, Goyal and Chu [9]. The so-called ‘‘fountain flow’’ effect describes the phenomena of polymer molecules near the centreline slowing down as they approach the melt front, reorienting towards the wall (orthogonal to the flow direction) and stretching as the charge surface is going backward, following a curved trajectory (Figure 4). According to the numerical investigation of Mavridis [8], the shear stresses are very large in the area affected by the fountain flow effect. With this in mind, it was assumed, that the pressure changes in the region far behind the melt front are considerably lower than in the area influenced by the fountain flow. In particular, the pressure rapidly drops to zero in this region (because the pressure immediately in the front of melt front is equal to zero). Therefore, the compression pressure as a function of the x coordinate can be approximately described as two regions of constant gradient, practically neglecting the shear stresses away from the region of fountain flow influence (Figure 5).

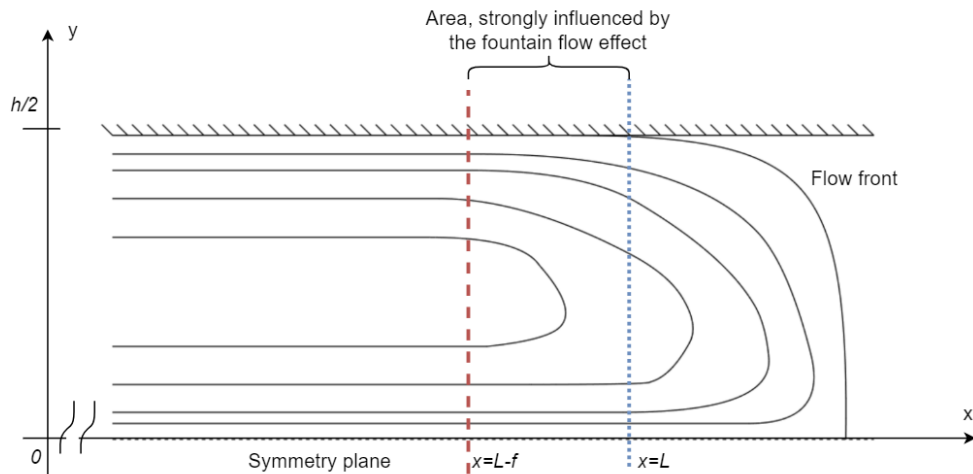


Figure 4: Schematic representation of the fountain flow phenomena [8]

According to the numerical and experimental investigation of the compression moulding process conducted by Mavridis [10], the length of the region impacted by the fountain flow effect increases with the decrease of gap height. The most intuitive and simple formulation of this dependency is as inverse proportionality. Further, considering constant volume of a charge, it can be determined, that the length of the material flow is in fact inversely proportional to the gap height:

$$V = LBh = Ah = \text{const} \quad (5)$$

$$L = \frac{V}{Bh} \quad (6)$$

Therefore, the length of the fountain flow impact region f (Figure 4) may be formulated as:

$$f = kL = \frac{kV}{Bh} \quad (7)$$

where, k is the dimensionless proportionality coefficient. Therefore, the wall shear stress at $x = L$ becomes:

$$\tau_w^L = \frac{h p_0}{2 f} = \frac{Bh^2 p_0}{2kV}, \quad (8)$$

and the hydrostatic compression pressure can be calculated as follows:

$$p_0 = \frac{F}{A} \quad (9)$$

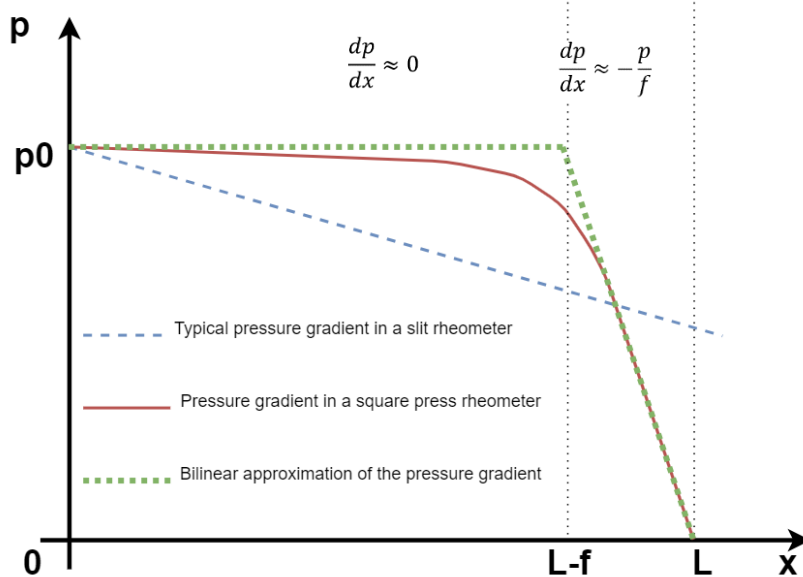


Figure 5: Pressure gradient in a square press rheometer as a function of x -coordinate along the line $(x, -\frac{h}{2})$ in Figure 3.

Using equations (5), (6) and (9), the relation (8) can then be formulated as:

$$\tau_w^L = \frac{FBh^3}{2kV^2}. \quad (10)$$

2.2 Shear rate

The typical velocity profile of a Newtonian fluid between two parallel plates is believed to be parabolic [16] (Figure 6). As such, the exact solution of a one-dimensional problem at the plane $(x, y) = (L, y)$:

$$v^L = v^L(y) = -\frac{4v_{max}^L}{h^2}y^2 + v_{max}^L, \quad \text{for } y \in \left[-\frac{h}{2}, \frac{h}{2}\right] \quad (11)$$

Accordingly, the first derivative of the function can be determined as a linear function of y :

$$\frac{dv^L}{dy} = -\frac{8v_{max}^L}{h^2}y \quad (12)$$

which is also the general definition of the shear rate of a fluid flow [2]:

$$\dot{\gamma} = \frac{dv}{dy}. \quad (13)$$

Therefore, the magnitude of the wall shear rate at the same plane $(x, y) = (L, y)$ is equal to:

$$\dot{\gamma}_{n,w}^L = \left| \frac{dv^L}{dy} \Big|_{y=h/2} \right| = \left| -\frac{8v_{max}^L}{h^2}y \Big|_{y=h/2} \right| = \frac{4v_{max}^L}{h} \quad (14)$$

Hence the relationship between $v_{average}$ and v_{max} is:

$$v_{average}^L = \frac{1}{h} \int_{-h/2}^{h/2} v^L dy = \frac{2}{h} \int_0^{h/2} \left(-\frac{4v_{max}^L}{h^2}y^2 + v_{max}^L \right) dy = \frac{2v_{max}^L}{3} \quad (15)$$

or

$$v_{max}^L = \frac{3v_{average}^L}{2} \quad (16)$$

Differentiating equation (6), $v_{average}^L$ can be related to v_{press} as follows:

$$\frac{dL}{dt} = v_{average}^L = -\frac{V}{Bh^2} \frac{dh}{dt} = \frac{Vv_{press}}{Bh^2} \quad (17)$$

Considering relations (16) and (17), equation (14) then becomes:

$$\dot{\gamma}_{n,w}^L = \frac{6v_{average}^L}{h} = \frac{6Vv_{press}}{Bh^3} \quad (18)$$

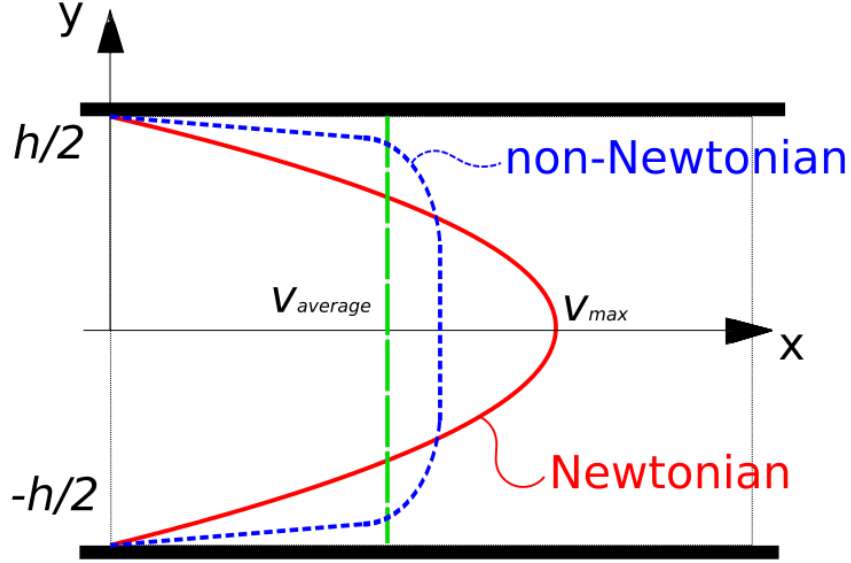


Figure 6: Schematic illustration of velocity profiles of a Newtonian and a non-Newtonian fluid with the same average velocity

Since fiber reinforced plastic melt does not belong to the group of Newtonian fluids, its velocity profile could not be considered as a parabola. Rather, its behaviour is hard to predict, and it depends on the fluid [11] (for example, one possible form is demonstrated in Figure 6. Consequently, the real value of the wall shear rate needs to be corrected using the Weissenberg-Rabinowitsch-Money correction analogue to the case of flow in a slit rheometer [7, 12]:

$$\dot{\gamma}_w^L = \frac{\dot{\gamma}_{n,w}^L}{3} \left[2 + \frac{d(\ln \dot{\gamma}_{n,w}^L)}{d(\ln \tau_w^L)} \right] \quad (19)$$

Finally, the material viscosity for given temperature can be computed according to its primary definition:

$$\eta = \frac{\tau_w^L}{\dot{\gamma}_w^L} \quad (20)$$

2.3 Temperature dependency

The mathematics in the two previous sections allows for the formulation of the viscosity as a function of shear rate under isothermal conditions. However, the real process is not isothermal and the viscosity is highly dependent on temperature. Therefore, to be able to use the measured data for any realistic simulations, it is important to formulate the temperature dependency function. A widely used approach for the issue uses the Williams-Landel-Ferry equation [13]:

$$\lg(\eta_0(T)) = \lg(D) + \left(\frac{-C_1(T - T_r)}{C_2 + (T - T_r)} \right), \quad (21)$$

where, η_0 is the material viscosity under zero shear condition (zero-shear-viscosity) as a function of temperature, D . C_1 and C_2 are free parameters that should be defined experimentally, and T_r is a reference temperature that needs to be selected.

Van Krevelen [14] recommends choosing $T_r = T_g + 43K$, where T_g is the glass transition temperature of the polymer being investigated. For this case, the parameters C_1 and C_2 are very similar for almost all amorphous polymers and equal to 9.51 and 94.6, respectively, which, in turn, allows conducting only a single viscosity measurement experiment to determine the temperature-shear dependency.

In the case that a polymer does not follow the typical C_1 and C_2 constants, the parameters still can be defined experimentally by choosing any suitable charge temperature as the reference temperature. Since three unknowns (D , C_1 , and C_2) are to be fitted, three experiments using different temperatures are needed.

3. Results

The materials used for simulation and experimental validation were PA6 (Ultrad® 8202HS) provided by BASF and glass fiber (StarRov 886) provided by Johns Manville. For the purpose of this study Ultrad® 8202HS and StarRov 886 were processed using the LFT-D line at the Fraunhofer Project Center, as shown schematically in Figure 1, to provide 30wt% glass LFT-D charges. These charges were then pressed into plaques and the process data was recorded. Samples of the charges were also sent to Moldex3D, Taiwan for characterization. The data recorded by the press is presented in Figures 7 and 8.

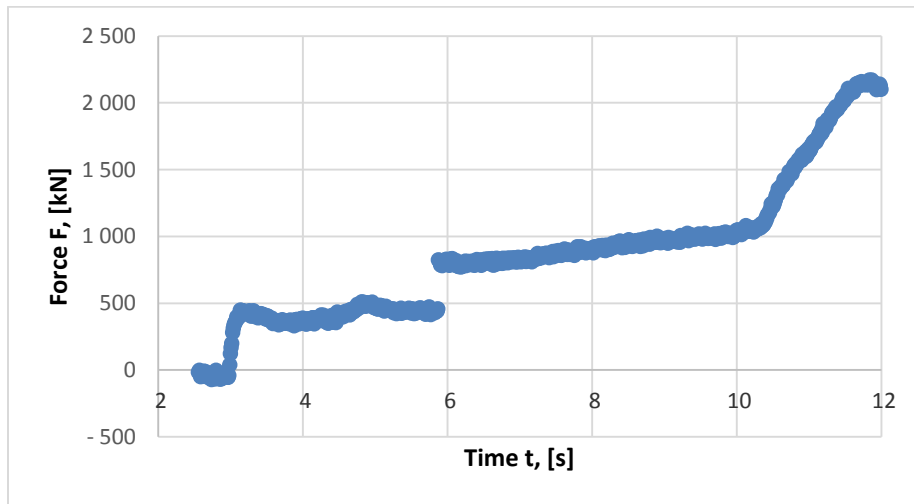


Figure 7: Force/Time measurement during compression

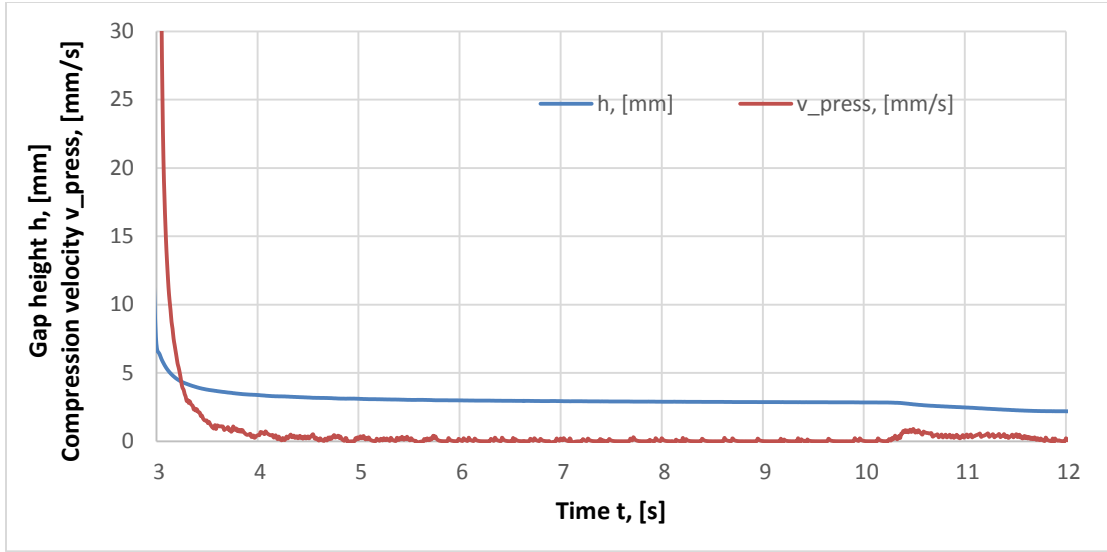


Figure 8: Gap/Time measurement during compression

Using the equations described in the second section and data obtained from Figures 7 and 8, the shear dependent viscosity was calculated. As shown in Figure 9, the viscosity calculated using the method suggested in this paper is compared with the viscosity measured by Moldex3D in their laboratory.

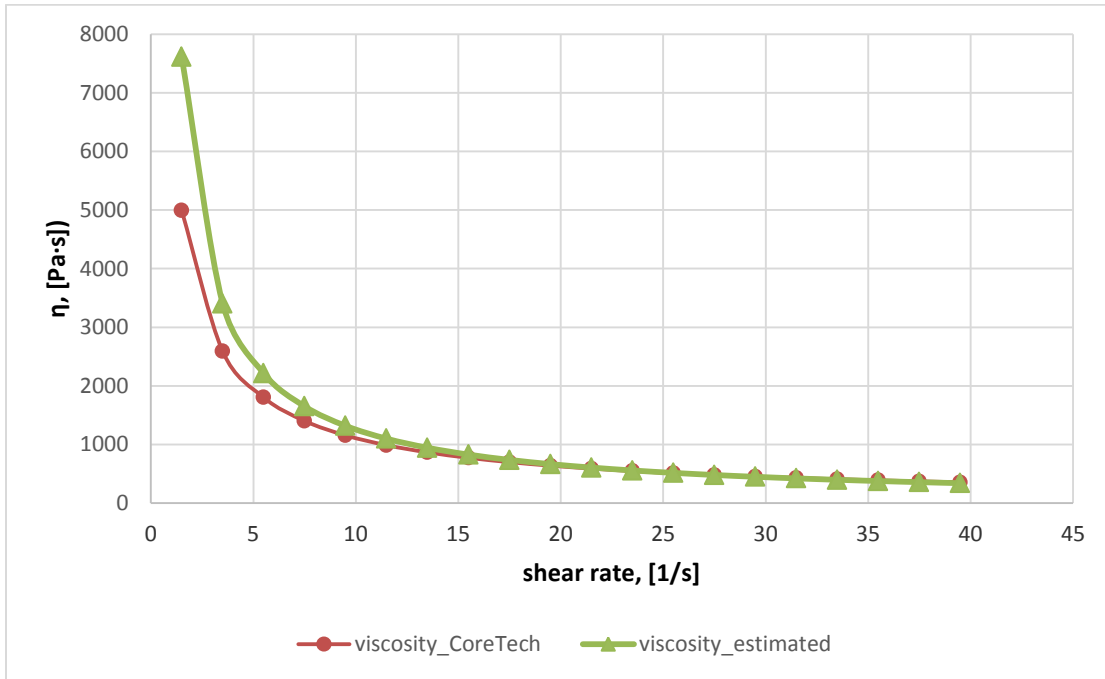


Figure 9: Comparison of viscosity measured by proposed method to viscosity measured by Moldex3D

4. Conclusions

A new method is proposed for the prediction (measurement and fast calculation) of the viscosity of LFT-D materials. The viscosity obtained by the proposed method matches well with the viscosity as measured by the Moldex3D laboratory, which is known to characterize the material correctly as simulations conducted using the data correlate well to that obtained from actual moldings. Hence, it is evident that the proposed method could be applied to LFT-D materials.

5. Acknowledgments

The present research was supported by the Natural Sciences and Engineering Research Council of Canada (NSERC) through the Automotive Partnership Canada (APC) program and industrial support from General Motors of Canada Ltd. (GMCL), BASF, Johns Manville (JM), Dieffenbacher North America (DNA) and Elring-Klinger. The authors would like to thank Louis Kaptur from DNA and all those at the Fraunhofer Project Center for their efforts in manufacturing the materials examined in this study.

6. References

- [1] H. Schürmann, Konstruieren mit Faser-Kunststoff-Verbunden, 2., bearbeitete und erweiterte Auflage, Berlin, Heidelberg: Springer Berlin Heidelberg, 2007.
- [2] W. Krause, F. Henning, S. Tröster, O. Geiger and P. Eyrer, "LFT-D – A Process Technology for Large Scale Production of Fiber Reinforced Thermoplastic Components," *Journal of Thermoplastic Composite Materials*, vol. 16, pp. 289-302, 2003.
- [3] J. Engmann, C. Servais and A. S. Burbidge, "Squeeze flow theory and applications to rheometry: A review," *Journal of Non-Newtonian Fluid Mechanics*, vol. 132, pp. 1-27, 2005.
- [4] F. Irgens, "Generalized Newtonian Fluids," in *Rheology and Non-Newtonian Fluids*, Cham, Springer International Publishing, 2014, pp. 113-124.
- [5] D. M. Kaylon, H. S. Tang and B. Karuv, "Squeeze Flow Rheometry for Rheological Characterization of Energetic Formulations," *Journal of Energetic Materials*, vol. 24, p. 195–212, 2006.
- [6] F. Wafzig, Konstruktion eines Press-Rheometers zur Charakterisierung von Faserverbundschmelzen, Diplomarbeit, Fachhochschule Kaiserslautern, 2007.
- [7] C. W. Macosko, *Rheology : Principles, Measurements, and Applications*, New York ; Weinheim: Wiley-VCH, 1994.
- [8] H. Mavridis, A. N. Hrymak und J. Vlachopoulos, „The Effect of Fountain Flow on Molecular Orientation in Injection Molding,“ *Journal of Rheology*, Bd. 32, p. 639, 1988.
- [9] M. R. Kamal, S. K. Goyal und E. Chu, „Simulation of Injection Mold Filling of Viscoelastic Polymer with Fountain Flow,“ *AIChE Journal*, Bd. 34, Nr. 1, pp. 94-106, 1988.
- [10] H. Mavridis, G. D. Bruce, G. J. Vancso, G. C. Weatherly und J. Vlachopoulos, „Deformation patterns in the compression of polypropylene disks: Experiments and simulation,“ *Journal of Rheology*, Bd. 36, Nr. 27, pp. 27-43, 1992.
- [11] J. Spurk and N. Aksel, "Laminare Schichtenströmungen," in *Strömungslehre: Einführung in die Theorie der Strömungen*, 9. Auflage, Berlin, Springer Vieweg, 2019, pp. 181-221.
- [12] P. Guillot and A. Colin, "Determination of the flow curve of complex fluids using the Rabinowitsch–Mooney equation in sensorless microrheometer," *Microfluidics and Nanofluidics*, vol. 17, no. 3, p. 605–611, 2014.
- [13] M. L. Williams, R. F. Landel und J. D. Ferry, „The Temperature Dependence of Relaxation Mechanisms in Amorphous Polymers and Other Glass-forming Liquids,“ *Journal of the American Chemical Society*, Bd. 77, Nr. 14, p. 3701–3707, 1955.
- [14] D. W. van Krevelen, revised by K. te Nijenhuis, *Properties of Polymers: their Correlation with Chemical Structure; their Numerical Estimation and Prediction from Additive Group Contributions*, 4th, completely revised edition, Amsterdam: Elsevier, 2009.